RNA (1997), 3:577–585. Cambridge University Press. Printed in the USA.

Ribonuclease P RNA: Models of the 15/16 bulge from *Escherichia coli* and the P15 stem loop of *Bacillus subtilis*

THOMAS R. EASTERWOOD[1] and STEPHEN C. HARVEY

Department of Biochemistry & Molecular Genetics, University of Alabama at Birmingham, Birmingham, Alabama 35294, USA

ABSTRACT

The *Escherichia coli* ribonuclease P RNA 15/16 internal bulge loop and the *Bacillus subtilis* P15 stem loop are important substrate binding sites for the CCA-3′ terminus of pre-tRNA. Models of *E. coli* 15/16 bulge loop and the *B. subtilis* P15 stem loop have been constructed using MC-SYM, a constraint satisfaction program. The models use covariation analysis data for suggesting initial base pairings, chemical probing, and protection/modification results to determine particular pairing orientations, and mutational experimental analysis data for tRNA-RNase P RNA contacts. The structures from *E. coli* and *B. subtilis*, although different in secondary structure, have similar sequence and function. Using MC-SYM, we are able to illustrate how the 3′ end of the pre-tRNA is able to interact with this segment of the catalytic RNase P RNA. In addition, we propose additional hydrogen bonding between A76 in the 3′ terminus of the tRNA and the 15/16 region of *E. coli* and to the loop of *B. subtilis*.

Keywords: bulge loop; MC-SYM; noncanonical base pairs; RNase P RNA; stem loop; tRNA

INTRODUCTION

Ribonuclease P (RNase P) is a catalytic RNA that cleaves the 5′ leader strand from pre-tRNA to produce a mature tRNA. The *Escherichia coli* RNase P consists of two parts, a 14-kDa protein known as the C5 protein, and a 377-nt RNA known as the M1 RNA (Kirsebom, 1995). The M1 RNA has been shown to be the catalytic portion of the molecule (Guerrier-Takada et al., 1983).

Within the RNase P RNA is a conserved sequence, present in *E. coli* as a bilateral, asymmetric bulge between helices P15 and P16, as represented in Figure 1. This conserved sequence is also present in *Bacillus subtilis*, but forms a stem loop at P15, instead of a bulge loop junction, as shown in Figure 1. This conserved sequence has been shown to be important in binding the 3′ end of pre-tRNA. LaGrandeur et al. (1994) were able to show protection of the conserved region from chemical modification when the CCA-3′ end of the tRNA was present. The protections indicated that specific interactions were occurring between the 3′ acceptor end and the bulge loop. Oh and Pace (1994) demonstrated through crosslinking that the 3′ end of the tRNA was directed toward helix P16. In addition, Kirsebom and Svärd (1994), through mutational analysis, showed that cleavage of the 5′ leader sequence was aberrant when the 15/16 bulge loop sequence was altered. The aberrant RNase P RNA could be rescued by mutating the tRNA ACCA 3′ end to be complimentary to the mutated bulge loop.

Models of the overall structure of the M1 RNA have been proposed by Westhof and Altman (1994) and Harris et al. (1994). The Westhof and Altman model was constructed initially as helices and stem loops at the all-atom level of detail using a computer. The parts were then assembled and optimized to alleviate inappropriate bond lengths, angles, and torsions. In the Westhof and Altman model, several contacts are indicated between the pre-tRNA and the catalytic M1 RNA. Among the contacts are those between the tRNA acceptor stem (ACCA-3′ end) and the bulge loop between helices P15 and P16. Westhof and Altman propose that A73-C74 at the 3′ end of tRNA are paired to U294-G293 as per Kirsebom and Svärd (1994). Be-

Reprint requests to: Stephen C. Harvey, Department of Biochemistry & Molecular Genetics, University of Alabama at Birmingham, Basic Health Sciences Building, Room 552, 1918 University Blvd., Birmingham, Alabama 35294, USA; e-mail: harvey@neptune.cmc.uab.edu.

[1]Current address: Southeastern Bible College, 3001 Hwy. 280 E., Birmingham, Alabama 35243, USA.

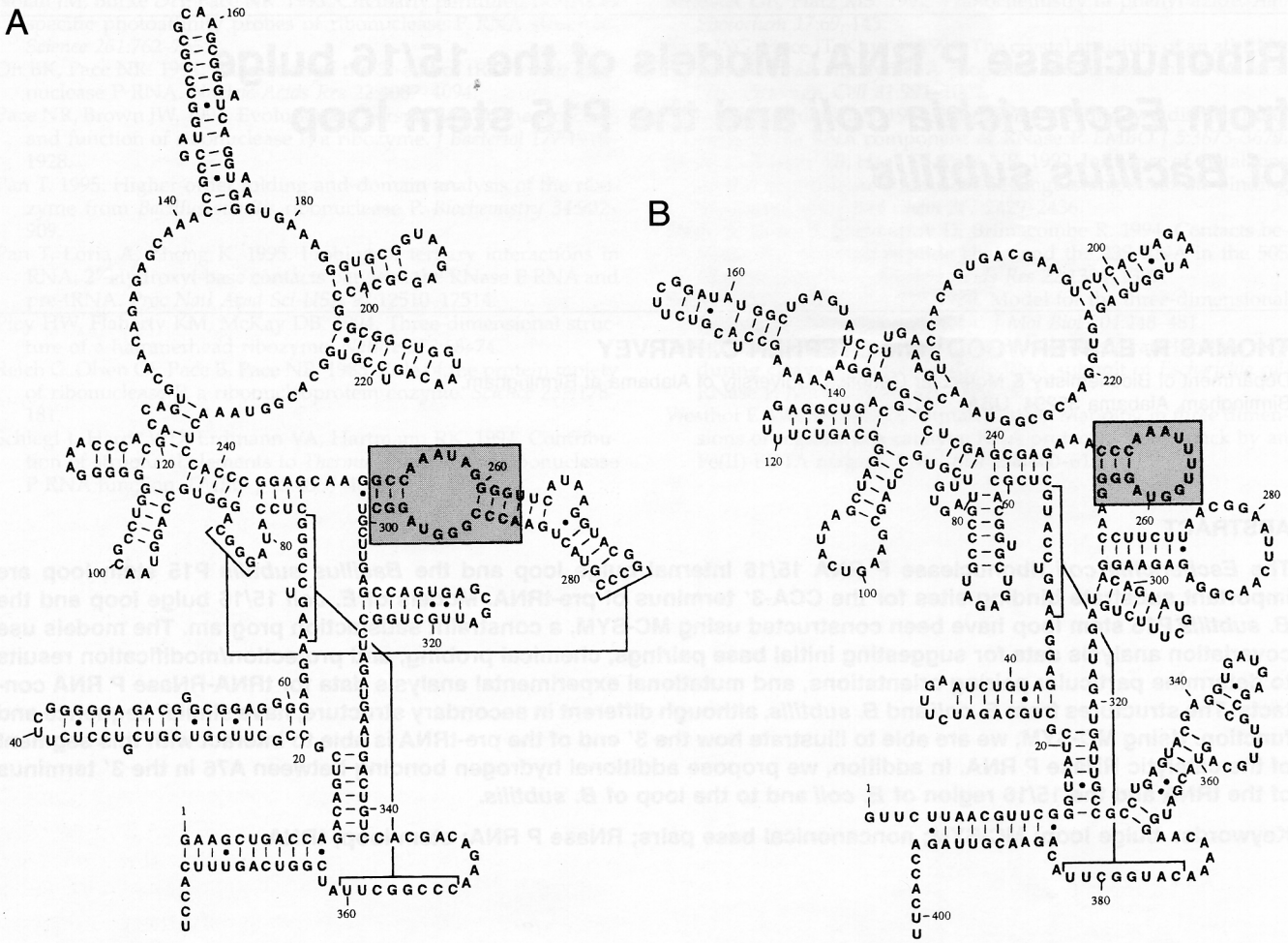

FIGURE 1. Secondary structure of RNase P RNA. **A:** *E. coli* RNase P RNA with the P15/16 bulge loop in the shaded box. **B:** *B. subtilis* RNase P RNA with the P15 stem loop in the shaded box.

cause of these base pairings, it was necessary to melt the acceptor stem of the pre-tRNA in the Westhof and Altman (1994) model so that contacts to the 5′ end of the tRNA could also be satisfied. Instead of using all atoms, the Harris et al. (1994) RNase P RNA model was constructed using a pseudo-atom approach, which approximates the position of nucleotides. The model was refined using a modification of YAMMP (Malhotra et al., 1990, 1994; Tan & Harvey, 1993; Malhotra & Harvey, 1994), a molecular mechanics package. The overall structure of the Harris et al. model is more compact than the Westhof and Altman model. The compact nature of the Harris et al. model allows the acceptor stem of the pre-tRNA to remain folded, while satisfying the contacts between the tRNA and RNase P RNA. Comparable contacts are seen in the Harris et al. model as in the Westhof and Altman model (i.e., the ACCA-3′ end of the pre-tRNA contacts the 15/16 bulge region).

The *E. coli* 15/16 bulge loop and the *B. subtilis* P15 stem loop have several nucleotides in common. The common sequence and functional significance of the segment should lend itself to a similar structure. In addition, a similarity in contacts between the two structures and the tRNA 3′ end should occur based upon this phylogenetic comparison.

We propose all-atom models of the *E. coli* 15/16 asymmetric bulge and the *B. subtilis* P15 stem loop. The models were constructed using MC-SYM's search capabilities, which allowed us to test various pairings and conformations for each nucleotide (Major et al., 1991, 1993; Gautheret & Cedergren, 1993). The models incorporate the covariation analysis data (Brown et al., 1996) shown in Figure 2, which we take to suggest several noncanonical pairings between the nucleotides in the two strands of the *E. coli* bulge. The models also incorporate modification/protection data (LaGrandeur et al., 1994; Oh & Pace, 1994) shown in Figure 3, giving the proper orientation of the proposed noncanonical pairings. The models produced by MC-SYM agree with the results of the mutational analysis (Kirsebom & Svärd, 1994), and indicate a possible noncanonical pairing between A76 and G259 in the *E. coli* RNase P RNA.

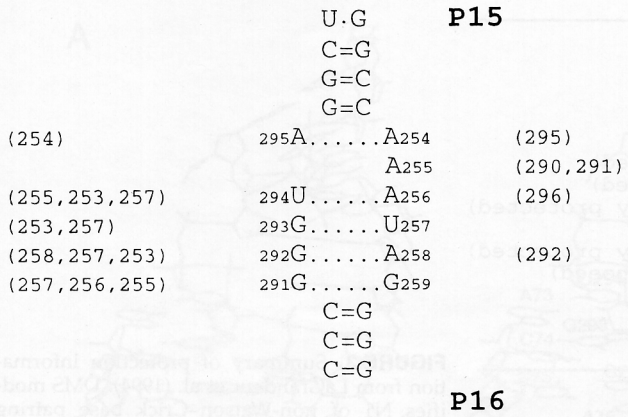

FIGURE 2. Proposed pairings for the *E. coli* bulge. The *E. coli* bulge with the nucleotide numbering scheme is represented in the center with helix P15 at top and helix P16 at the bottom. Numbers in parentheses represent the sequence numbering of nucleotides in the opposite strand, which covary with the nucleotide indicated. The numbers are from our observation of the top five covariation analysis M values (Brown et al., 1996). The pairings we have proposed are represented by dots across the bulge. Actual M values from the covariation data do not confirm the pairings but were used to suggest initial pairings for our MC-SYM search.

RESULTS

In the structures modeled here, we have made certain assumptions that limit the number of nucleotide conformations searched in MC-SYM, allowing for faster search times and preventing runaway searches (Major et al., 1991, 1993; Gautheret & Cedergren, 1993). We attempted to maintain typical A form (C3′ *endo* ribose sugar pucker) nucleotide backbone conformation in our nucleotides, because this is standard for most RNA structures. However, for the *B. subtilis* model, we have used B-form C2′ *endo anti* nucleotide conformations in the loop tips, because this is common in RNA stem loops (Varani, 1995, and references therein). We have avoided the use of *syn* base conformations in the construction of our models because they are less common in RNA structure than the *anti* base forms. We can also increase the speed of the search procedure employed by MC-SYM by avoiding *syn* base conformational sets. Protections presented in the LaGrandeur et al. (1994) data for bases in the *E. coli* RNase P 15/16 bulge indicate some interaction with other parts of the RNase P. Because the two strands of the bulge are in obvious proximity to each other, we have used mutual covariation analysis data from Brown et al. (1996) to suggest possible base pairings across the *E. coli* 15/16 bulge.

E. coli bulge model

In our *E. coli* MC-SYM search, 30 structures were obtained when the information from Figure 3 was used to eliminate inappropriate conformations. By further limiting the conformational sets, eliminating inappropriate base pairings, and decreasing the distances for O3′ and P connectivity, we were able to arrive at one structure. Nucleotides C74 and C75, representing the tRNA acceptor 3′ end, were modeled as Watson–Crick base pairs to G293 and G292. Not only were the base pairs feasible, agreeing with the mutational analysis of Kirsebom and Svärd (1994), but the resulting orientation was that determined by Oh and Pace (1994) with the 3′ end of the tRNA acceptor directed toward helix P16, as illustrated in Figure 4. The addition of A76 to the C74-C75 chain indicated a potential noncanonical pairing between A76 and G259. The orientation of the A76-G259 base pairing is shown in Figure 4. The pairing does explain the protection of G259 by A76 and the modification observed when tRNA with A76 removed is bound to the *E. coli* RNase P RNA (LaGrandeur et al., 1994). Although we have not modeled the tRNA acceptor stem helix in our structure, there is ample room for the construction of the helix (data not shown). The conformation of the bulge and the curvature of the CCA would indicate that the ribose–phosphate backbone of the pre-tRNA acceptor stem helix interacts with A254 and A255 in a nonspecific manner. The chemical probing data and the results with mutational analysis in the A254-A255 region indicate that an interaction is occurring here, although the specificity of the interaction cannot be identified conclusively from the data (Kirsebom & Svärd, 1994).

We tested pairings for A73 in the tRNA and A256 in RNase P RNA to U294. We found that three pairings are possible at this position. A U294 to A256 Watson–Crick pair can be formed and satisfy the protection/modification data in Figure 3 (LaGrandeur et al., 1994). In addition, a U294-tRNA A73 Watson–Crick pair can also be formed as proposed by Kirsebom and Svärd (1994). A third orientation for U294, somewhat between the tRNA pair and the RNase P RNA pair, is also possible, as shown in Figure 5. This third configuration contains one hydrogen bond between U294 and A73. A second hydrogen bond also occurs between N6 of A256 and O4 of U294. The final structure in Figure 4 represents a synthesis of all experimental data and is perhaps the best representation of the present state of the data.

B. subtilis stem loop model

We have assumed the same base pairings in the *B. subtilis* model as we used for the *E. coli* structure based upon the covariation analysis data (Brown et al., 1996). The assumption of similar pairings is based upon similar sequence in the two secondary structures. Because of the pairings imposed on the *B. subtilis* loop, the loop tip forms a tetraloop-like structure. The predominance of three- and four-nucleotide RNA loops (Varani, 1995) make the assumed pairings reasonable. When we use the proposed pairings from covariation analysis for other species that exhibit a stem loop at P15, we find

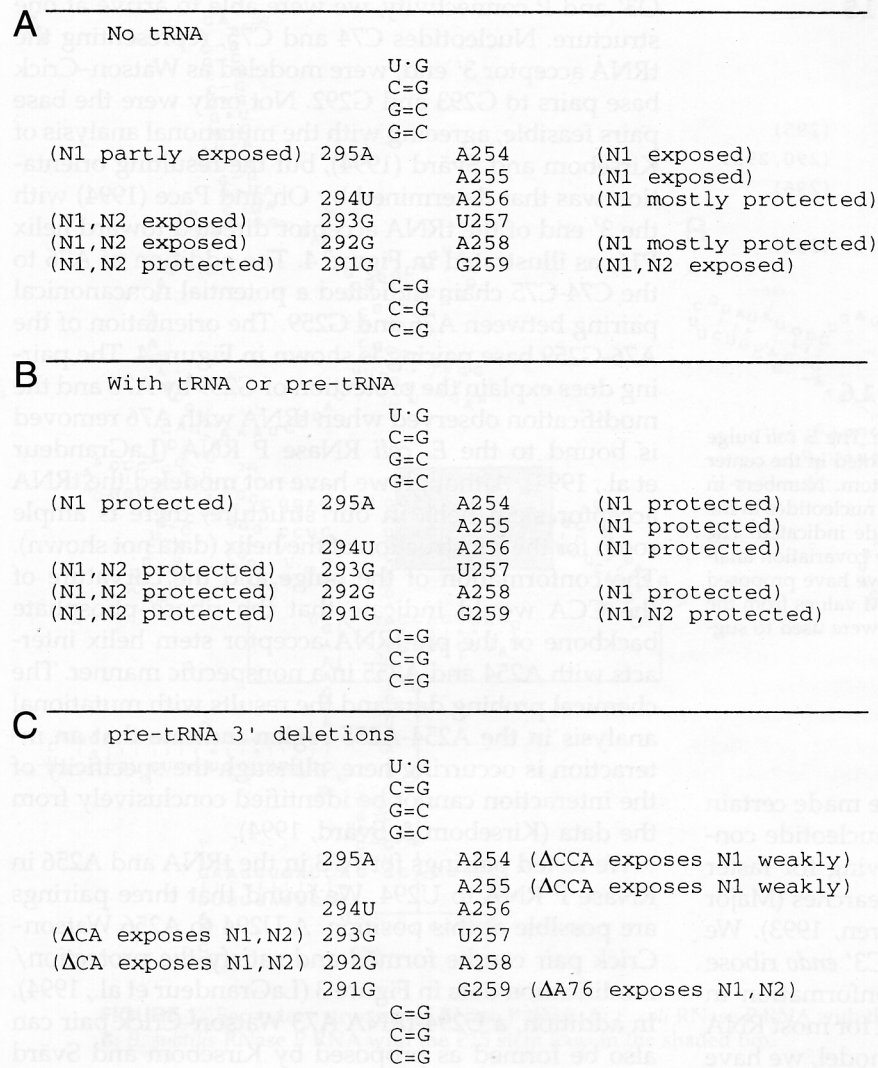

FIGURE 3. Summary of protection information from LaGrandeur et al. (1994). DMS modifies N1 of non-Watson–Crick base pairing adenines and kethoxal modifies N1 and N2 of non-Watson–Crick base pairing guanines. **A:** Protection/modification data, derived from RNase P RNA *without* the bound tRNA. **B:** Protection/modification data for the 15/16 bulge when tRNA or pre-tRNA is present and bound to the RNase P RNA. **C:** Protection/modification data for the 15/16 bulge when tRNA with various 3′ deletions (ΔA, tRNA-A76 is removed; ΔCA, tRNA-C75+A76 removed; ΔCCA, tRNA-C74+C75+A76 is removed) is bound to the RNase P RNA. Note the effect of deleting A76 on G259.

the majority of the secondary structures would be of a tetraloop nature. There is only one case, *Bacillus brevis*, in which the tetraloop configuration would not be feasible with the proposed pairings from the covariation data. However, in *B. brevis*, a three-nucleotide loop is possible while maintaining our proposed pairings (Brown & Pace, 1994).

The initial *B. subtilis* stem loop construction provided 30 structures from our MC-SYM search. All 30 of the conformations were very similar, with only minor variations in the ribose-phosphate backbone conformations distinguishing them. The particular orientation of base pairings were selected from the possible MC-SYM pairs based on the protection/modification data of LaGrandeur et al. (1994). Limiting the conformational sets, eliminating inappropriate base pairings, and decreasing the distances between O3′ and P allowed us to limit the collection to one structure.

The final structure in Figure 4 is the result of our MC-SYM search and selection procedures. Pairing of *B. subtilis* A261-A251 in Figure 5 is similar to that of *E. coli* A295-A254, except that the pairing is reversed based upon the LaGrandeur et al. (1994) chemical modification/protection data. The A261-A251 base pairing provides greater protection of N1 of A251, as indicated in the modification/protection data of LaGrandeur et al. (1994). We have Watson–Crick paired U260 to A253. The loop tip is similar to, but not exactly the same as, a UUUG tetraloop (Cheong et al., 1990) in that the loop is closed with a noncanonical G-U base pair between U255 and G258. There is a single hydrogen bond from N3 of U255 to N7 of G258. Nucleotides U256 and U257 use B-type C3′ *endo* sugar conformations because A-type conformations could not be used to close the loop. The presence of B-type sugar pucker in the loop is consistent with observed RNA loop structure (Puglisi et al. 1990). Nucleotides G259 and G258, which base pair to C74 and C75 in the tRNA 3′ acceptor strand, present the appropriate base pairing faces for the interaction. An interesting result on adding the tRNA nt A76 to our *B. subtilis* structure is that A76 has the potential to Watson–Crick pair with U257 in the loop.

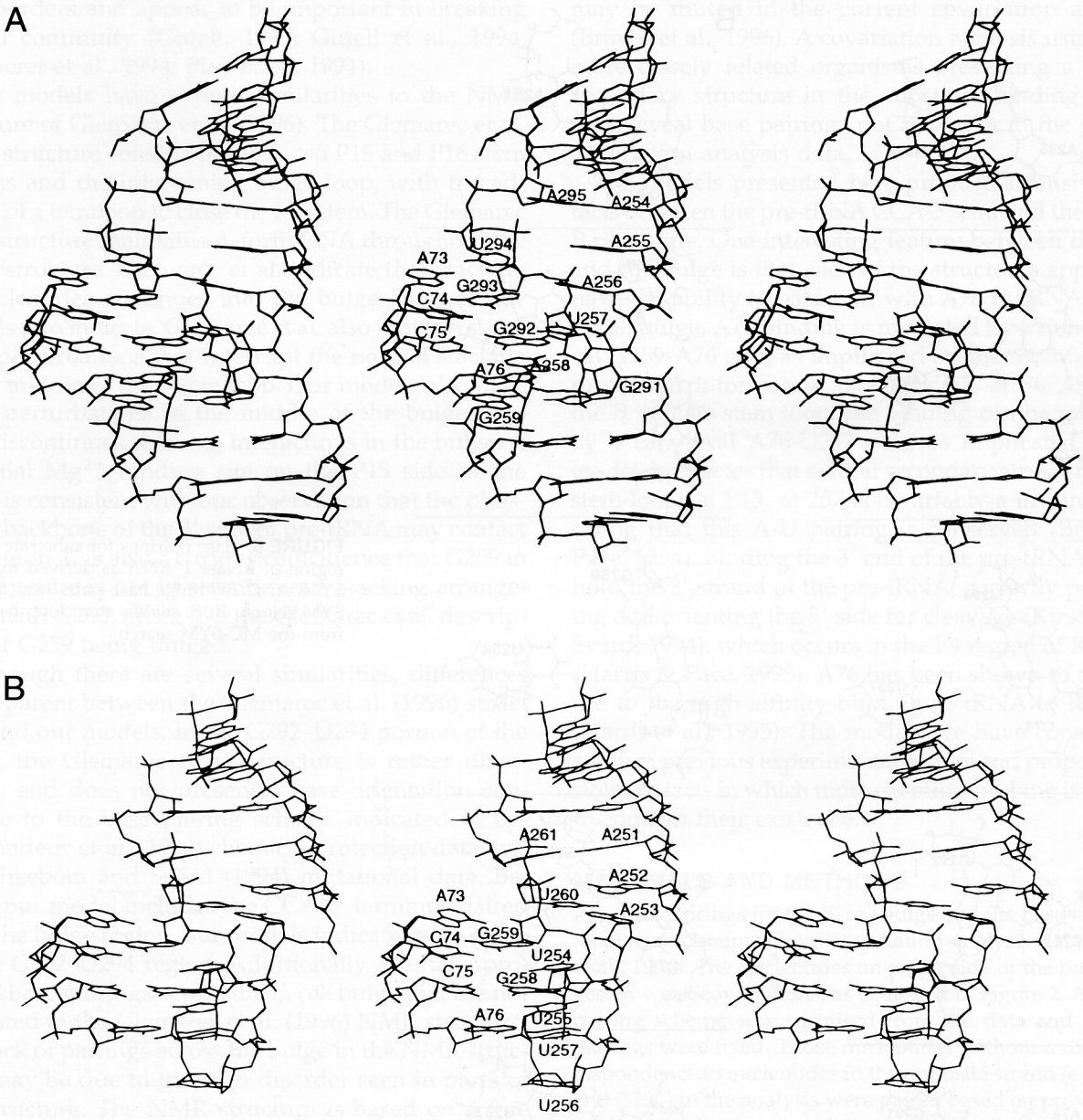

FIGURE 4. Stereo triple images of the modeled substrate binding region of RNase P RNA. The left pair is the convergent view, and the right pair is the divergent view. **A**: Image of the *E. coli* bulge as derived from MC-SYM with helix P15 at the top and helix P16 at the bottom. Nucleotides in the bulge are numbered, as are the ACCA representing the 3′ end of the tRNA. Note the position of A76 and its position relative to G259. **B:** Image of the *B. subtilis* stem loop as derived from MC-SYM with helix P15 at the top. The nucleotides in the loop are numbered, as is the ACCA representing the 3′ end of the tRNA. Again, note the position of A76 toward the bottom and its pairing with U257.

DISCUSSION

It is evident from the phylogenetic conservation of sequence and chemical probing data that the 15/16 bulge in *E. coli* and the P15 stem loop of *B. subtilis* are important for binding and holding the CCA 3′ terminus of pre-tRNA. The mutational analysis (Kirsebom & Svärd, 1994) shows that this highly conserved RNase P RNA sequence is necessary to position the pre-tRNA correctly so that processing and cleavage can occur at the proper site on the 5′ side of the acceptor stem. Chemical probing data (LaGrandeur et al., 1994) also indicates the close interaction between the pre-tRNA CCA-3′ end and the RNase P RNA 15/16 bulge. Although the order of processing in prokaryotes (3′ or 5′ first) is unknown, the processing order should not be a factor in the binding of the ACCA-3′ end of tRNA to the 15/16 bulge, because ACCA is encoded in the gene for many *E. coli* tRNAs. Our models also indicate that the phosphate backbones may be in close contact in the bulge region, which allows the proper orientation of nucleotide bases for base pairing to the ACCA ter-

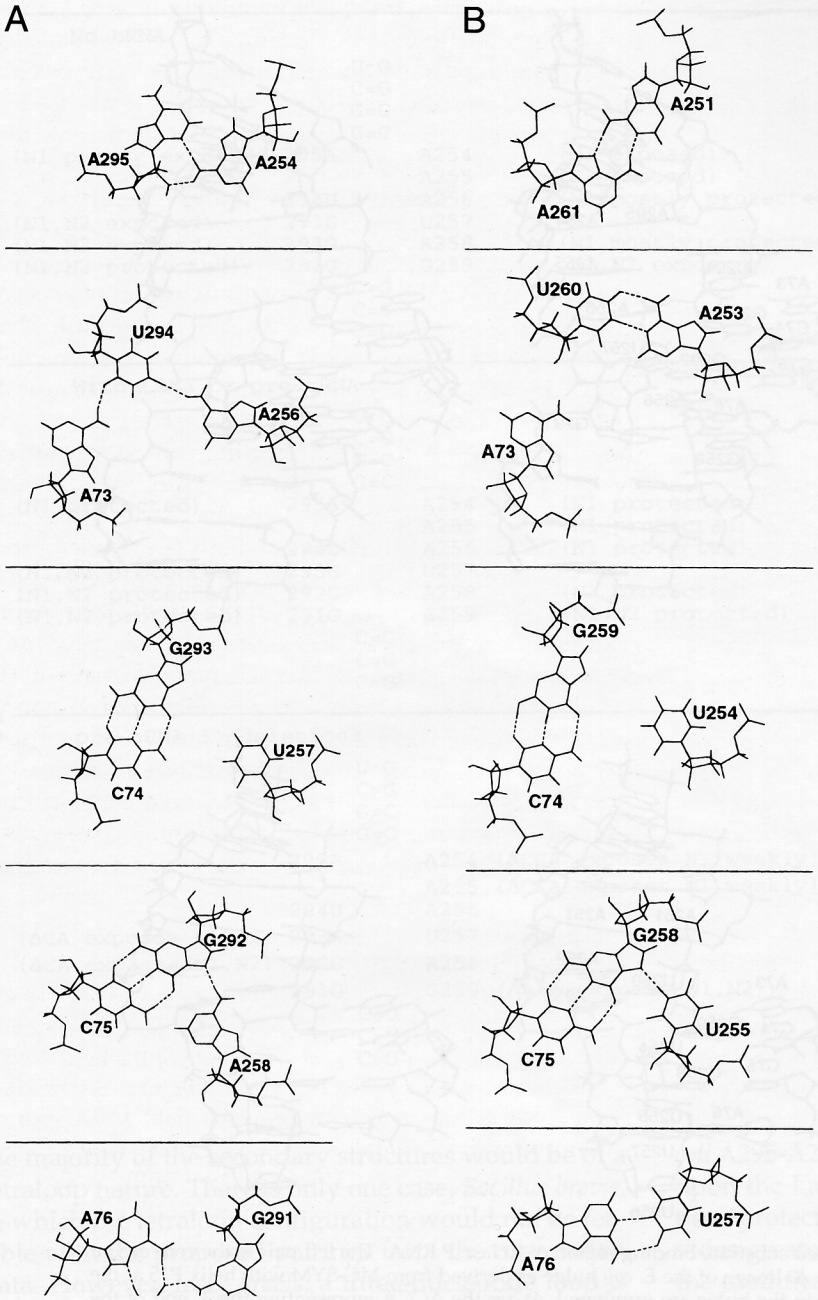

FIGURE 5. Base pairings for substrate binding region of RNase P RNA as derived from MC-SYM. **A:** *E. coli* bulge base pairs from the MC-SYM search. **B:** *B. subtilis* stem loop base pairs from the MC-SYM search.

minus. The necessity of high magnesium concentrations to achieve active RNase P RNA in the absence of protein indicates that the protein may be involved in negating electrostatic repulsion caused by the close approach of phosphates in the RNase P RNA structure (Darr et al., 1992).

The binding of the pre-tRNA 3′ end to RNase P RNA is mediated by a different secondary structure in the two organisms, although the sequence in each is similar. Both the *E. coli* bulge loop and the *B. subtilis* stem loop have identical sequences in the P15 helix (excepting the inversion of the initial GC pair). They also have similar sequences in the 5′-AAAU region of the J15/16 bulge, and the 5′-GGUA on the J16/15 side of the bulge. This particular sequence is very common among the various RNase P sequences available presently (Brown & Pace, 1994), demonstrating the loop's strong link to function. In both the bulge and the loop, the presence of noncanonical base pairs would allow the exposure of appropriate functional groups for the performance of the base pairing function in this region. Noncanonical AA pairings in the *B. subtilis* loop and *E. coli* bulge, along with the closure of the *E. coli* bulge by noncanonical AG and GG pairs, are consistent with a pattern in bulge and loop borders. The noncanonical GA, AA, or GG pairs tend to be abundant in bulge and

loop borders and appear to be important in breaking helical continuity (Gutell, 1993; Gutell et al., 1994; Gautheret et al., 1994; Pley et al., 1994).

Our models have several similarities to the NMR structure of Glemarec et al. (1996). The Glemarec et al. NMR structure consists of the *E. coli* P15 and P16 stem regions and the intervening bulge loop, with the addition of a tetraloop to close the P16 stem. The Glemarec et al. structure maintains A-form RNA throughout the bulge structure. Glemarec et al. indicate that stacking of nucleotides continues into the bulge loop, as our models also indicate. Glemarec et al. also indicate structural perturbations that interrupt the normal stacking in the middle of the bulge loop. Our models also have some perturbations in the middle of the bulge loop that discontinues stacking interactions in the bulge. A potential Mg^{2+} binding site on the P15 side of the bulge is consistent with our observation that the phosphate backbone of the 3′ side of pre-tRNA may contact this region. It is also a curious coincidence that G259 in our structure is not in a continuous stacking arrangement with G260, much like the Glemarec et al. description of G259 being bulged.

Although there are several similarities, differences are apparent between the Glemarec et al. (1996) structure and our models. In the G292–U294 portion of the bulge, the Glemarec et al. structure is rather disordered, and does not present a base orientation conducive to the base pairing scheme indicated in the LaGrandeur et al. (1994) chemical protection data and the Kirsebom and Svärd (1994) mutational data. Because our model includes the CCA-3′ terminus paired with the bulge region, our models indicate more order in the G292–U294 region. Additionally, we have proposed base pairings across the *E. coli* bulge that are not indicated in the Glemarec et al. (1996) NMR structure. The lack of pairings across the bulge in the NMR structure may be due to the high disorder seen in parts of the structure. The NMR structure is based on a free structure out of the context of the intact RNase P RNA. Our pairings across the loop are based on chemical protections from intact RNase P RNA (LaGrandeur et al., 1994) and covariation analysis data (Brown et al., 1996). The protection data not attributable to the presence of the CCA-3′ terminus of the pre-tRNA is likely due to interactions with RNase P RNA. Because the most proximal portion of RNase P RNA would be the opposing strand in the loop, we have sought to satisfy protection data not attributed to CCA-3′ pre-tRNA with noncanonical base pairs across the loop. The data from the covariation analysis (Brown et al., 1996) for each position in the bulge do not confirm the base pairings. However, because the substrate binding region in the different species used in the covariation analysis have varying numbers of nucleotides in their lengths, as well as different secondary structure presentations (bulge or stem loops), base pairings within the bulge may be muted in the current covariation analysis (Brown et al., 1996). A covariation analysis using only more closely related organisms presenting a similar secondary structure in the substrate binding region may reveal base pairings not apparent in the present covariation analysis data.

The models presented here propose extensive contacts between the pre-tRNA CCA-3′ end and the RNase P ribozyme. One interesting feature between the loop and the bulge is that each of the structures appears to have the ability to base pair with A76 in tRNA. In the *E. coli* bulge, A76 binding is mediated by a noncanonical G259-A76 pair, as implicated by the modification/protection information (LaGrandeur et al., 1994). In the *B. subtilis* stem loop, the binding can be mediated by a canonical A76-U257 pair, as implicated in our model. In species that exhibit secondary structures with stem loops at P15, nt 257 is invariably a uridine, indicating that this A-U pairing is conserved (Brown & Pace, 1994). Binding the 3′ end of the pre-tRNA would hold the 3′ strand of the pre-tRNA, correctly positioning and orienting the 5′ side for cleavage (Kirsebom & Svärd, 1994), which occurs in the P4 region of RNase P (Harris & Pace, 1995). A76 has been shown to contribute to the high-affinity binding of tRNA to RNase P (Hardt et al., 1995). The models we have constructed confirm previous experimental results and propose possible contacts in which more chemical probing is needed to confirm their existence.

MATERIALS AND METHODS

Potential pairings for the *E. coli* bulge and the *B. subtilis* stem loop were obtained from covariation analysis data (Brown et al., 1996). The nucleotides on either side of the bulge suggested weak covariations, as exhibited in Figure 2. An initial pairing scheme was surmised from the data and the best pairings were fixed. Those nucleotides without a direct correspondence to nucleotides in the opposite strand (e.g., G259 and G291) in the analysis were paired based on proximity to nucleotides in the opposite strand. The final pairings for U294 with A255 and A256 were determined using MC-SYM's ability to build the structure (Major et al., 1991, 1993; Gautheret & Cedergren, 1993) and the agreement of the resulting structures with the protection/modification information shown in Figure 3 (LaGrandeur et al., 1994). We assumed throughout the building process typical C3′ endo *anti* nucleotide conformations, except in cases where C2′ endo conformations have been indicated previously (i.e., the *B. subtilis* loop; see Cheong et al., 1990; Puglisi et al., 1990; Varani, 1995).

To determine the base orientations in each of the pairings (i.e., Watson–Crick, Hoogsteen, or other noncanonical pairs), we used MC-SYM to search for possibilities. First, helix P16 was constructed in MC-SYM, and G291 was stacked on the 3′ side of helix P16. G259 was allowed to sample various pairings with G291 using MC-SYM. MC-SYM allows 24 possibilities for GG base pairings. The constraints of connection to the 3′ side of the helical ribose phosphate backbone limits the number of possibilities available to the GG pairing. We

utilized only C3′ *endo* nucleotide conformations, which also limited the number of possible final structures. From the results of the base pairing search, we selected those that gave the best agreement with the chemical probing data (LaGrandeur et al. 1994).

Each of the other pairings in the bulge were searched in a manner similar to that of the G259-G291 pair, proceeding one nucleotide pair at a time toward the P15 helix. A258 was stacked on G259 and G292 was allowed to sample base pairings to A258. G293 was stacked on G292 and U257 was allowed to sample base pairings to G293. A255 and A256 were each tested for possible pairings to U294. Base pairings between U294 and A255 were not in agreement with the chemical probing data. In addition, construction of a base pair between U294 and A255 was difficult, especially in making the ribose-phosphate backbone connections. The A256 and U294 trial pairing formed a good Watson-Crick base pair, making the proper connections with the ribose phosphate backbone, and, in the process, satisfying the chemical probing data. To help close the bulge, A254 was stacked on A255 and A295 was allowed to sample base pairings with A254. Lastly, helix P15 was constructed, finishing the *E. coli* bulge. We also began the *E. coli* construction with the P15 helix and, using the approach described above, were successful in constructing the bulge loop with the same types of pairings observed when beginning from the P16 helix.

The final step in constructing the *E. coli* bulge was to add the ACCA-3′ acceptor end to the structure. MC-SYM was employed to Watson-Crick pair C74 to G293. Then C75 was Watson-Crick paired to G292. The connection between the 5′ P of C75 and the 3′ OH of C74 were reasonable based on our selected MC-SYM adjacency constraint of 5.1 Å. The pairings agree with the chemical probing data (LaGrandeur et al., 1994; Oh & Pace, 1994) and with the mutational analysis (Kirsebom & Svärd, 1994). A76 was connected to C75 in an A-type helical conformation. After examining the structures, the J15/16 side of the bulge was rebuilt to allow for better closure between O3′ of A256 and P of U257. Additional searches were performed for pairings between A256 and U294, as well as pairings between U294 and tRNA nt A73 to arrive at the final structure. MC-SYM searches were also made for base pairing between A76 and G259 and the best pairing agreement with probing data was selected from among the results.

The construction of the *B. subtilis* stem loop was performed in a manner similar to that of *E. coli*. Beginning with helix P15, we explored various pairings, as in the *E. coli* construct. The closure of the loop required a U254 to G258 pairing in place of the *E. coli* A258 to G292 pairing. The construction of the ACCA 3′ segment on the stem loop was done as in the *E. coli* bulge, pairing C74 and C75 to G259 and G258, respectively. A76 was added in a type A RNA conformation to C75. A73 was also added to C74 in a type A RNA conformation. In the *B. subtilis* structure, we did not perform further searches on the possible pairing between U260 and A73. Those pairings best matching the LaGrandeur et al. (1994) data were chosen from the resulting possibilities.

Both structures were adjusted manually to bring the O3′-P backbone contacts into proper arrangement. The structures were then subjected to 200 steps of steepest-descent minimization without electrostatics using Sybyl, a Tripos, Inc. modeling package, to alleviate inappropriate bond lengths, angles, torsions, and steric contacts. A final 200 steps of steepest-descent minimization were performed on the models with electrostatics to complete the clean-up of the models.

NOTE ADDED IN PROOF

The structures proposed here have been incorporated into the model for the complete ribozyme/substrate structure proposed by Harris et al. (pages 561–576 in this issue).

ACKNOWLEDGMENTS

We thank Norm Pace for helpful discussions, Jim Nolan for providing the results of the covariation analysis data, and Jim Brown for discussions about the significance of the covariation data in the *E. coli* bulge. Special thanks to Michael Harris for his insightful discussions and his knowledge of RNase P RNA. Supported by NIH grant GM-53827.

Received November 25, 1996; returned for revision December 20, 1996; revised manuscript received March 31, 1997

REFERENCES

Brown JW, Nolan JM, Haas ES, Rubio MA, Major F, Pace NR. 1996. Comparative analysis of ribonuclease P RNA using gene sequences from natural microbial populations reveals tertiary structural elements. *Proc Natl Acad Sci USA 93*:3001–3006.

Brown JW, Pace NR. 1994. The ribonuclease P database. *Nucleic Acids Res 17*:3660–3662.

Cheong C, Varani G, Tinoco I Jr. 1990. Solution structure of an unusually stable RNA hairpin, 5′GGAC(UUCG)GUCC. *Nature 346*: 680–682.

Darr SC, Brown JW, Pace NR. 1992. The varieties of ribonuclease P. *Trends Biochem Sci 17*:178–182.

Gautheret D, Cedergren R. 1993. Modeling the three-dimensional structure of RNA. *FASEB J 7*:97–105.

Gautheret D, Konings D, Gutell RR. 1994. A major family of motifs involving G_A mismatches in ribosomal RNA. *J Mol Biol 242*:1–8.

Glemarec C, Kufel J, Földesi A, Maltseva T, Sandström A, Kirsebom LA, Chattopadhyaya J. 1996. The NMR structure of 31mer RNA domain of *Escherichia coli* RNase P RNA using its non-uniformly deuterium labelled counterpart [the "NMR-window" concept]. *Nucleic Acids Research 24*:2022–2035.

Guerrier-Takada C, Gardiner K, Marsh T, Pace N, Altman S. 1983. The RNA moiety of ribonuclease P is the catalytic subunit of the enzyme. *Cell 35*:849–857.

Gutell RR. 1993. Comparative studies of RNA: Inferring higher-order structure. *Curr Opin Struct Biol 3*:313–322.

Gutell RR, Larsen N, Woese CR. 1994. Lessons from an evolving rRNA: 16S and 23S rRNA structures from a comparative perspective. *Microbiol Rev 58*:10–26.

Hardt WF, Schlegl J, Erdmann VA, Hartmann RK. 1995. Kinetics and thermodynamics of the RNase P RNA cleavage reaction: Analysis of tRNA 3′-end variants. *J Mol Biol 247*:161–172.

Harris ME, Nolan JM, Malhotra A, Brown JW, Harvey SC, Pace NR. 1994. Use of photoaffinity crosslinking and molecular modeling to analyze the global architecture of ribonuclease P RNA. *EMBO J 13*:3953–3963.

Harris ME, Pace NR. 1995. Identification of phosphates involved in catalysis by the ribozyme RNase P RNA. *RNA 1*:210–218.

Kirsebom LA. 1995. RNase P—A "scarlet pimpernel." *Mol Microbiology 17*:411–420.

Kirsebom LA, Svärd SG. 1994. Base pairing between *Escherichia coli* RNase P RNA and its substrate. *EMBO J 13*:4870–4876.

LaGrandeur TE, Hüttenhofer A, Noller HF, Pace NR. 1994. Phylogenetic comparative chemical footprint analysis of the inter-

action between ribonuclease P RNA and tRNA. *EMBO J 13*:3945–3952.

Major F, Gautheret D, Cedergren R. 1993. Reproducing the three-dimensional structure of a tRNA molecule from structural constraints. *Proc Natl Acad Sci USA 90*:9408–9412.

Major F, Turcotte M, Gautheret D, Lapalme G, Fillion E, Cedergren R. 1991. The combination of symbolic and numerical computation for three-dimensional modeling of RNA. *Science 253*:1255–1260.

Malhotra A, Harvey SC. 1994. A quantitative model of the *Escherichia coli* 16 S RNA in the 30 S ribosomal subunit. *J Mol Biol 240*:308–340.

Malhotra A, Tan RKZ, Harvey SC. 1990. Prediction of the three-dimensional structure of *Escherichia coli* 30S ribosomal subunit: A molecular mechanics approach. *Proc Natl Acad Sci USA 87*:1950–1954.

Malhotra A, Tan RKZ, Harvey SC. 1994. Modeling large RNAs and ribonucleoprotein particles using molecular mechanics techniques. *Biophys J 66*:1777–1795.

Oh BK, Pace NR. 1994. Interaction of the 3′-end of tRNA with ribonuclease P RNA. *Nucleic Acids Res 22*:4087–4094.

Pley HW, Flaherty KM, McKay DB. 1994. Three-dimensional structure of a hammerhead ribozyme. *Nature 372*:68–74.

Puglisi JD, Wyatt JR, Tinoco I Jr. 1990. Solution conformation of an RNA hairpin loop. *Biochemistry 29*:4215–4226.

Tan RKZ, Harvey SC. 1993. Yammp: Development of a molecular mechanics program using the modular programming method. *J Comp Chem 14*:455–470.

Varani G. 1995. Exceptionally stable nucleic acid hairpins. *Annu Rev Biophys Biomol Struct 24*:379–404.

Westhof E, Altman S. 1994. Three-dimensional working model of M1 RNA, the catalytic RNA subunit of ribonuclease P from *Escherichia coli*. *Proc Natl Acad Sci USA 91*:5133–5137.